Report on

Characterization of metal/dielectric multilayers with in-situ ellipsometry

By Dao Hua ZHANG

Summary

The project was completed on 31 December 2010. In this project, we did simulations for metal/dielectric multilayer structures, their applications as hyperlens for sub-wavelength imaging with resolution beyond diffraction limit, optimized metal (silver) films and started fabrication and characterization of dielectric films with in-situ ellipsometry monitoring the thickness and optical constants. We numerically demonstrated that three dimensional imaging hyperlens with resolution of about 75 nm could be achieved. We submitted invention application in Sep. 2010. While our patent application was in press, Prof Xiang Zhang's group in UC Berkley reported a hyperlens with resolution of about 135 nm in Nature Communication on 21 Dec. 2010. We also simulated multilayer structures for other superlens applications. In the experimental aspect, we have systematically investigated silver films fabricated at different preparation conditions and effects of thickness on their properties. High quality silver films with root-mean-square roughness of about 0.9 nm were achieved. We also found that the dielectric constant of the silver films is sensitive to the thickness and the real part of the constant becomes positive when the silver film is as thin as 5 nm. This finding is very important to the application of the silver films in nanophotonic devices including superlens for high resolution imaging. In addition, the fabrication and characterization for dielectric films has also carried out. Multilayer hyperlens and other type of superlens will be fabricated and characterized once the characterization of the dielectric film is completed. So far, we have two papers accepted for presentation and the two papers will be published in the international journals, Applied Optics and Applied Physics A, respectively, after review.

1.   Introduction

Metamaterials consisting of metal/dielectric multilayers have been attracting great attention in the recent a few years due to their novel properties which do not exist in nature. Such metamaterials have many potential novel applications and hyperlens is probably the most exciting and promising application to date. It is well known that optical microscopy is the most widely used imaging method at present but the resolution of the conventional optics is constrained by diffraction limit which prevents imaging of subwavelength features and is considered as a fundamental barrier. Recent theoretical research revealed that hyperlens made of metamaterials could overcome the diffraction barrier. This lens would not only capture evanescent fields to retrieve sub wavelength information but also allow for their processing with standard optical components. About two years ago, Professor X. Zhang's laboratory at

Report Documentation Page

Public reporting burden for the collection of information is estimated to average 1 hour per response, including the time for reviewing instructions, searching existing data sources, gathering and maintaining the data needed, and completing and reviewing the collection of information. Send comments regarding this burden estimate or any other aspect of this collection of information, including suggestions for reducing this burden, to Washington Headquarters Services, Directorate for Information Operations and Reports, 1215 Jefferson Davis Highway, Suite 1204, Arlington VA 22202-4302. Respondents should be aware that notwithstanding any other provision of law, no person shall be subject to a penalty for failing to comply with a collection of information if it does not display a currently valid OMB control number.

1. REPORT DATE	2. REPORT TYPE	3. DATES COVERED
04 MAR 2011	**Final**	**17-06-2009 to 17-01-2011**

4. TITLE AND SUBTITLE	5a. CONTRACT NUMBER
Characterization of metal/dielectric multilayers with in-situ ellipsometry	**FA23860914083**
	5b. GRANT NUMBER
	5c. PROGRAM ELEMENT NUMBER

6. AUTHOR(S)	5d. PROJECT NUMBER
Dao Hua Zhang	
	5e. TASK NUMBER
	5f. WORK UNIT NUMBER

7. PERFORMING ORGANIZATION NAME(S) AND ADDRESS(ES)	8. PERFORMING ORGANIZATION REPORT NUMBER
Nanyang Technological University,Nanyang Avenue,639798,Singapore,NA,NA	**N/A**

9. SPONSORING/MONITORING AGENCY NAME(S) AND ADDRESS(ES)	10. SPONSOR/MONITOR'S ACRONYM(S)
AOARD, UNIT 45002, APO, AP, 96338-5002	**AOARD**
	11. SPONSOR/MONITOR'S REPORT NUMBER(S)
	AOARD-094083

12. DISTRIBUTION/AVAILABILITY STATEMENT
Approved for public release; distribution unlimited

13. SUPPLEMENTARY NOTES

14. ABSTRACT
In this project, metal/dielectric multilayer structures and their applications as hyperlenses for sub-wavelength imaging with resolution beyond diffraction limit were simulated and optimized. Fabrication and characterization of dielectric films with in-situ ellipsometry monitoring the thickness and optical constants has been started. Three dimensional imaging hyperlens with resolution of about 75 nm has been demonstrated numerically.

15. SUBJECT TERMS
meta materials, Materials Characterization

16. SECURITY CLASSIFICATION OF:			17. LIMITATION OF ABSTRACT	18. NUMBER OF PAGES	19a. NAME OF RESPONSIBLE PERSON
a. REPORT **unclassified**	b. ABSTRACT **unclassified**	c. THIS PAGE **unclassified**	**Same as Report (SAR)**	**11**	

University of California, Berkeley, experimentally fabricated cylindrical hyperlens made of Silver/Al_2O_3 multilayers, which indeed breaks the diffraction limit by magnifying the sub-diffraction-limited objects and projecting the magnified images to the far field. On 20 May 2009, his group proposed a hyperlens with flat input and output planes to generate subdiffraction-limited arbitrary patterns and such hyperlens is achievable by simulation. One of the challenges faced currently for the hyperlens application is to find suitable metal and dielectric which can form metamaterials with suitable optical parameters. The other one is the precise control of the optical parameters of such metal and dielectric layers at nanometer scale dimension. In this project, we will simulate the multilayer structures for high resolution imaging, fabricate and characterize metal and dielectric films with the in-situ ellipsometry monitoring the thickness and optical constants so as to achieve high quality metal/dielectric multilayers for high resolution imaging.

2.   Results and discussion

2.1   Simulation and parameter optimization of hyperlens

We investigated methods that could be used to improve the performance of hyperlens with COMSOL numerical simulations tool. Theoretical analyses showed that the dispersion relation of the hyperlens could be tuned by adjusting its geometric parameters or by adjusting the permittivity of the metal-dielectric pairs and the resulting normalized power flow and beam divergence at the output of hyperlens were affected. Theoretical analyses and numerical simulations also showed that the 0° beam divergence could be achieved by optimizing the metal filling ratio or by tuning the permittivity of the metal-dielectric pairs. Simultaneously, the phase mismatch at the output of hyperlens could be eliminated when the 0° beam divergence condition was satisfied. The sub-wavelength resolution capability of the hyperlens can be improved by increasing its thickness, while the beam intensity decreases due to the increased material absorption in thicker hyperlens. For hyperlenses with equal thickness, increasing the number of split metal-dielectric layers improves the performance. This is a result of the increased splitting of surface plasmon (SP) modes as the number of layers increases. However, the performance cannot be improved indefinitely and it saturates as the number of periods reaches a critical level.

After some data were achieved, we extended the simulation into 3 dimensional domains. In the 3 dimensional domains the hyperlens becomes hemispherical shape. As a result of its geometry, the hemispherical hyperlens works on normally incidence light in any polarization direction. The hemispherical hyperlens isotropically magnifies the image details alone radial direction. In this work, we numerically demonstrate that images can be obtained by the hemispherical hyperlens under a rotational linearly polarized light.

2.1.1   One dimensional cylindrical hyperlens

Simulation of the cylindrical hyperlens was carried out first. The simulated hyperlens consists of 32 curved periodic stack (16 pairs) of Ag (ε_m=-2.4012+0.2488i) and Al2O3 (ε_m=3.217) deposited on a half-cylindrical quartz substrate (ε=2.174), with a single layer thickness of 50nm. The results showed that the optimized filling ratio evaluated in term of minimum full width at maximum (FWHM) (p=0.42) and maximum power flow (p=0.44) is close to the theoretically calculated value 0.4274 by ray trajectory analysis. At the optimized filling ratio, the 0° beam divergence and minimized phase mismatch can be achieved. The performance of the hyperlens can be improved by properly adjusting the metal filling ratio.
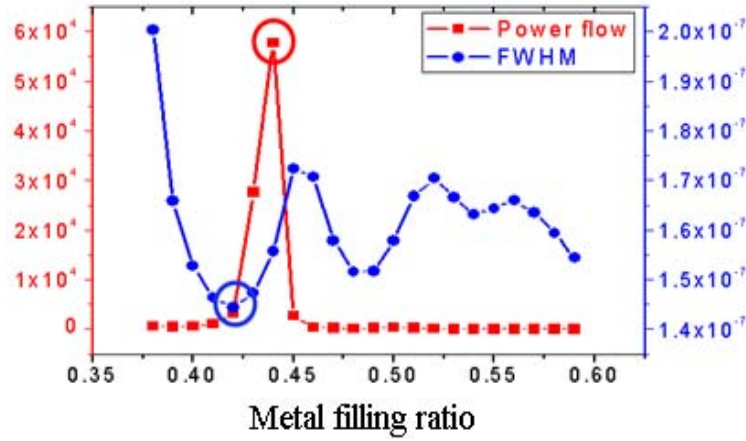
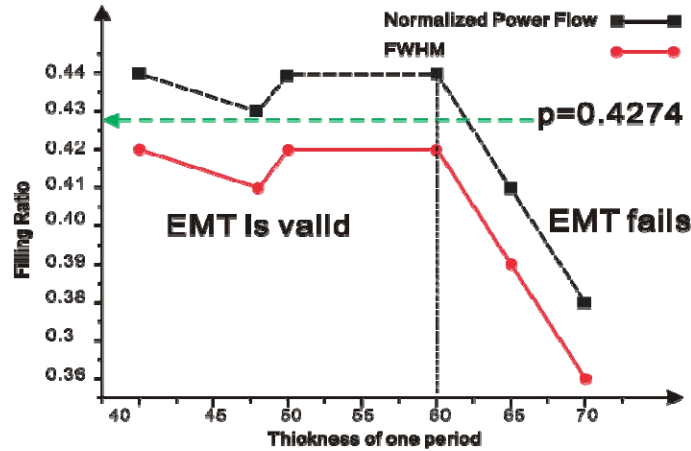Fig. 1. Filling ratio Vs. normalized power flow and FWHM.

Fig. 2. Optimized filling ratios of the hyperlens with different single layer Ag-Al$_2$O$_3$ thickness.

Our simulation also showed that the effective medium theory is only valid for hyperlens with single Ag-Al$_2$O$_3$ layer thinner than 60 nm. For hyperlens with single Ag-Al$_2$O$_3$ layer thickness beyond 60 nm, the simulation results diverge from the theoretically calculated value 0.4274.

The effect of increasing number of periods for hyperlens with same thickness has been investigated. In this case, the filling ratio is fixed at 0.5, the inner radius and outer radius of the hyperlens are 240nm and 1360nm respectively. The performance is evaluated in term of normalized power flow and FWHM.
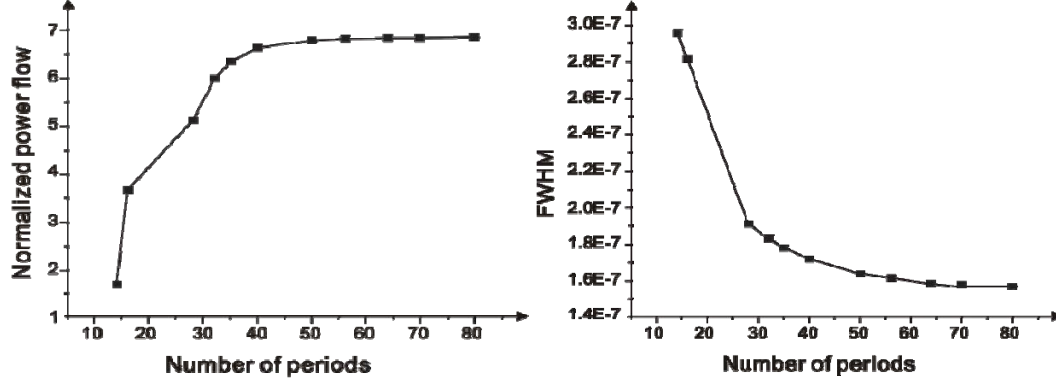
Fig. 3. Number of Ag-Al$_2$O$_3$ layers Vs. FWHM (left) and normalized power flow (right) evaluated at the output of the hyperlens.

Simulation results indicate that the performance of the hyperlens improves as the number of splitted metal-dielectric stacks increases. It can be explained by the splitting of surface plasmon modes in multilayer meta-dielectric structure. Microscopically, Sub-wavelength resolution capability of hyperlens is achieved by excitation of surface plasmons. Interaction of modes on two metal surfaces causes surface plasmon modes to split. As the number of metal thin films increases, the degree of the split surface plasmon modes increases accordingly. However, the simulation also shows that the improvement starts to saturate as the number of periods reaches a critical level. Thus in real device fabrication, the number of layers has to be designed carefully.

2.1.2 Three dimensional cylindrical hyperlens

For the cylindrical hyperlens, we extended the simulations into 3 dimensional spaces. Simulation results show that the fine features of the object is not magnified equally in all directions. Due to its cylindrical structure, the fine features of the object are magnified in the radial direction. While along the cylinder axis, the fine features are not magnified and a distorted image is obtained. Thus, the 3 dimensional cylindrical hyperlens works like a hyperlens in radial direction, while in cylinder axis direction it works like a cascaded superlens. As shown in the figure below, the images of these small holes are distorted.
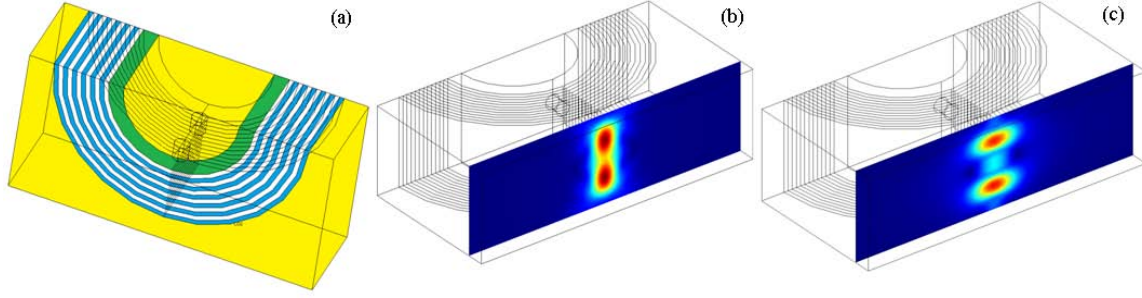
Fig. 4. (a) Illustration of the simulation structure, 2 small holes are opened along the direction of the cylinder axis (b) Image formed under TM illumination with H field along z-axis (c) Image formed under TE illumination with H field along x-axis.
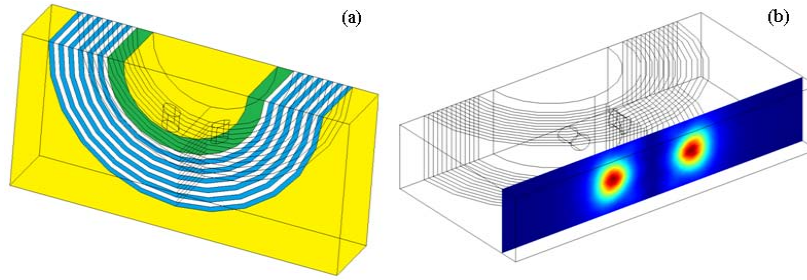

Fig. 5. (a) Illustration of the simulation structure, 2 small holes are opened along the direction normal to the cylinder axis (b) Image formed under TM illumination with H field along z-axis.

2.1.3   Hemispherical hyperlens

To overcome the limitations of the cylindrical hyperlens, 3 dimensional hemispherical hyperlens is proposed in this project. Beneficial from the hemispherical geometry, the 3 dimensional hemispherical hyperlens works on polarized light in any direction. In addition, the 3 dimensional hemispherical hyperlens isotropic magnifies all the wave information. This is a big improvement over the cylindrical hyperlens. In the numerical simulations, we create diffraction limited patterns at the input of the hyperlens. To simulate a rotational linearly polarized light, we used linearly polarized light with different polarization direction as the incident beam and superpose all the images obtained. At the output, images of the diffraction limited patterns are restored and magnified above the diffraction limit. Our numerical simulations showed that the 3 dimensional hemispherical hyperlens performs better than the cylindrical hyperlens.
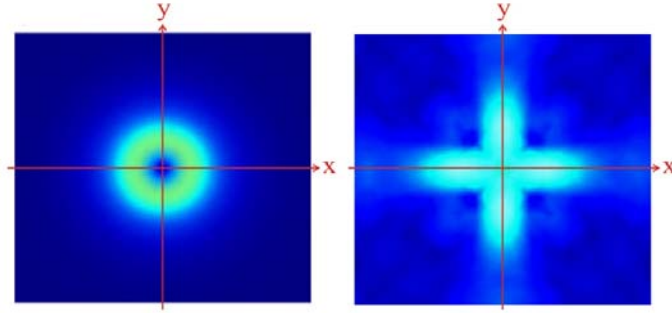
Fig. 6. Image of an annular ring with inner radius of 35 nm and outer radius of 65 nm (left); images of a cross with line width of 20 nm and length of 180 nm (right).

2.1.4   Fabrication of hemispherical hyperlens

Based on the numerical simulations, we are currently fabricating the hemispherical hyperlens. The major challenge will be the fabrication of the multilayer structure. Since there are many layers to be fabricated, sidewall coverage must be controlled as close as to bottom coverage. This could be achieved by using extremely low deposition rate. In real fabrication of the hyperlens, Zhang Xiang's group used electron beam evaporation deposition with deposition rate of 0.3nm/s, good sidewall coverage was achieved. In this project, sputter machine is used to deposit the metal-dielectric layers. Much lower deposition rate could be achieved by sputter machine. With the multi-target sputter machine, the multilayer metal-dielectrics could be fabricated in one run without opening the chamber. With all those advantages, the fabricated hyperlens should have better performance than the evaporated one. Our recent studies have been motivated to find an optimal deposition parameter which is able to not only produce an ultra-smooth Ag thin film, but also to improve its optical behaviors for metamaterials application.

2.2. Characterization of metal and dielectric films by in-situ ellipsometry and Atomic Force Microscopy

In this report, we also show our experimental results on surface roughness and the value of optical constants for Ag thin films produced directly on bare quartz glass by dc sputtering technique. The root-mean-square (rms) surface roughness, the thickness and optical constants of Ag films were studied by atomic force microscopy (AFM) and reflecting ellipsometry respectively.

2.2.1   Fabrication of silver films

All of our samples were deposited onto bare quartz substrates using self-designed multi-target magnetron sputtering system. A spectroscopic ellipsometer is integrated into the chamber which is able to carry out the in-situ measurements of Ag thin film's thickness and optical properties. The deposition was performed at room temperature from a 2-inch Ag metal target with a high

purity of 99.99% in pure argon ambient. The distance between the sputtered target and the quartz substrate is about 18 cm. Before deposition the quartz substrates are cleaned ultrasonically in acetone, IPA and then rinsed by DI water. The substrates are cleaned by dried nitrogen gas gun and placed immediately into the vacuum chamber. The sputtering chamber is evacuated by a turbo-molecular pump backed by a two-stage oil pump. Prior to the deposition, the chamber is pumped down to less than 5.0×10^{-6} mtorr. During the deposition, the substrate is floated without a dc-bias applied. To study the effects of sputtering parameters, all the samples are divided into 3 groups. In the first group, the thickness effect is investigated. The depositions are conducted in pure Ar ambient of 2 mtorr with an applied dc power of 20 W. The thicknesses of Ag thin films are 5 nm, 10 nm, 15 nm, 30 nm and 50 nm. And then the thickness of 50 nm is chosen for our next step of deposition optimization. In the second group, the sputtering pressure (P_{total}) is varied by adjusting the sputtering gas flow rate. The total pressure of the sputtering gas is regulated by mass-flow controller. In our work, five sputtering pressures of 1 mtorr, 2 mtorr, 5 mtorr, 10 mtorr and 20 mtorr were chosen for the thin film deposition with 20 W-forwarded dc powers. The corresponding deposition rates were calibrated to be 0.8929, 0.8418, 0.6983, 0.4562 and 0.1918 Å/s, respectively. Finally, five different values (10 W, 20 W, 30 W, 40 W and 50 W) of dc power were applied to investigate the forwarded power effects on surface roughness and optical properties. The deposition rates were calibrated to be 0.4010, 0.8418, 1.330, 1.8116 and 2.242 Å/s, respectively. Based on the calibration results, all the Ag thin films were maintained at an approximately same thickness (about 50 nm) for the characterizations.
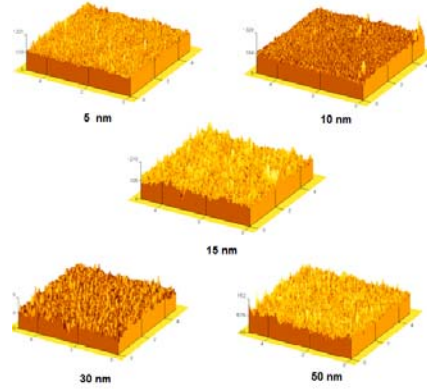
2.2.2   Surface roughness

Fig. 7 (a) shows the variation of surface roughness as a function of thickness of Ag thin films. The rms surface roughness measured for Ag thin films is 13.8 Å, 12 Å, 16 Å, 12.9 Å and 9.36 Å corresponding to 5 nm, 10 nm, 15 nm, 30 nm and 50 nm, respectively. It is showed that 50-nm thick Ag thin film has a best smooth surface. It is attributed to the silver's island-growth mechanism. At the beginning of thin film deposition, the island will be formed on the substrate. Thus the surface of Ag film is very rough which is showed in figure 1 (b). With the more Ag atoms reaching the surface of substrate, the continuous film will be formed and the surface of Ag thin film become more and more smooth. So when the thickness reached 50 nm, the rms roughness of Ag thin film is reduced from 13.8 Å to 9.36 Å.

Figure 8 and 9 illustrate the effects of sputtering pressure and forwarded power on surface roughness. The results show that at a certain conditions of 20 W and 2 mtorr, the silver thin film possesses an ultra-smooth surface.
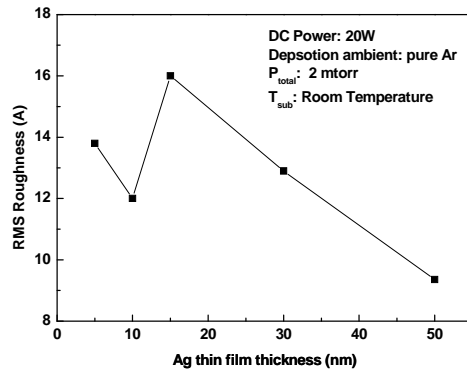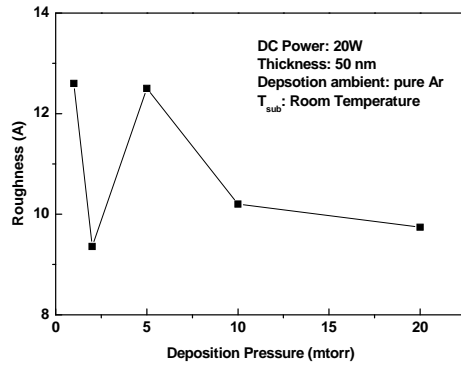
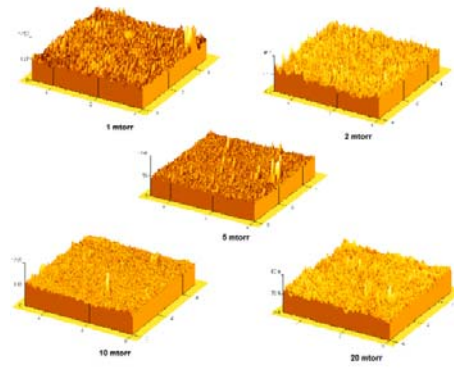(a)   (b)

Fig. 7(a) Variation of surface roughness as a function of thickness of Ag thin films (b) AFM 3-D images of Ag films with a thickness of 5 nm, 10 nm, 15 nm, 30 nm and 50nm. All the films are deposited in pure Ar ambient of 2 mtorr with a dc power of 20W.

(a)   (b)

Fig. 8. (a) Variation of surface roughness as a function of sputtering pressure (b) AFM 3-D images of Ag films deposited in a sputtering pressure of 1, 2, 5, 10 and 20 mtorr. All the films are deposited by a dc power of 20W with a thickness of 50 nm.
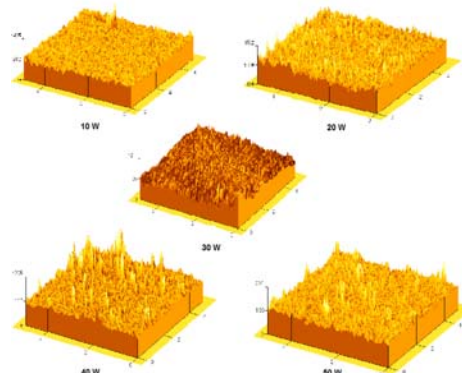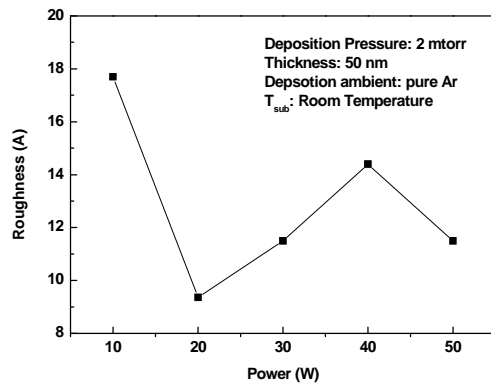
Fig. 9. (a) Variation of surface roughness as a function of forwarded dc power (b) AFM 3-D images of Ag films deposited with a dc power of 10, 20, 30, 40 and 50 Watt. All the films are deposited in pure Ar ambient of 2 mtorr with a thickness of 50 nm.

2. 2.3 Optical constant studies

The optical measurements were carried out in situ under UHV conditions in the frequency range 430-845 nm which can ensure the Ag films don't be oxided during the measurement. All of our data analysis was done in terms of the complex index of refraction $\tilde{n} = n + ik$. We will present what follows in terms of $\tilde{\varepsilon} = \varepsilon_1 + i\varepsilon_2$, however, as $\tilde{\varepsilon} = \tilde{n}^2$. In the thickness effect, we change the thickness from 5 nm to 1000 nm to study the variation of dielectric constants of Ag from thin film to bulk. The spectroscopic ellipsometry results show that the variation of ε_1 and ε_2 of Ag films as function of the thickness from thin film to bulk. It is also shown that the real part of permittivity of ultra-thin Ag film became positive with the thickness reduced to 5 nm. And the sputtering pressure and forwarded power effects are not significant compared to thickness effect that is obvious in Figure 10-12.
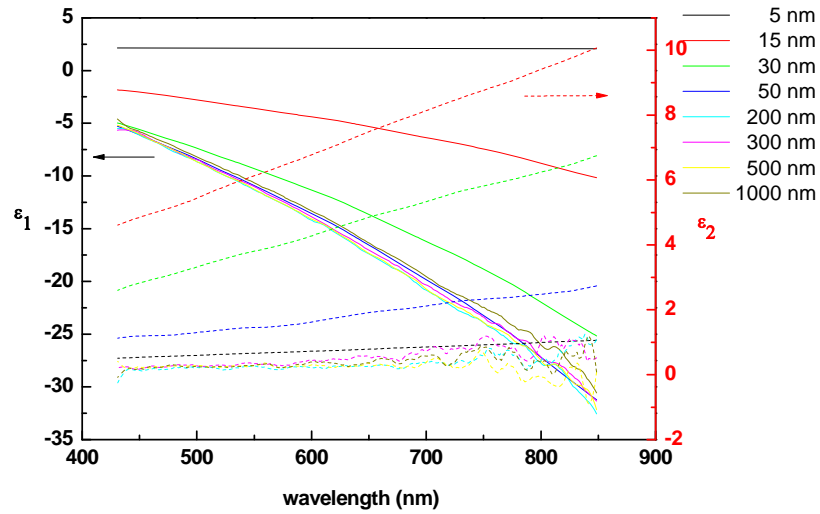

Fig. 10. The dielectric constant of ε_1 (left) and ε_2 (right) of Ag thin film as a function of thickness (5, 15, 30, 50, 100, 200, 300, 500 and 1000 nm).
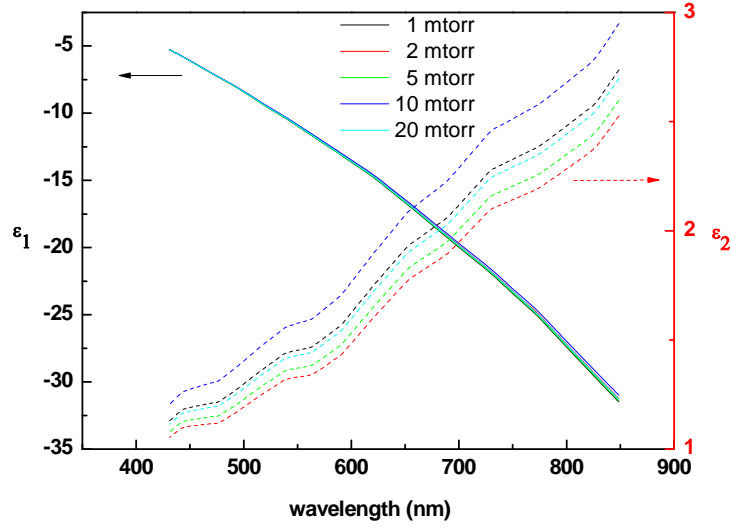
Fig. 11. The dielectric constant of ε_1 (left) and ε_2 (right) of 50 nm-thick Ag thin film as a function of the sputtering pressure of 1, 2, 5, 10 and 20 mtorr.
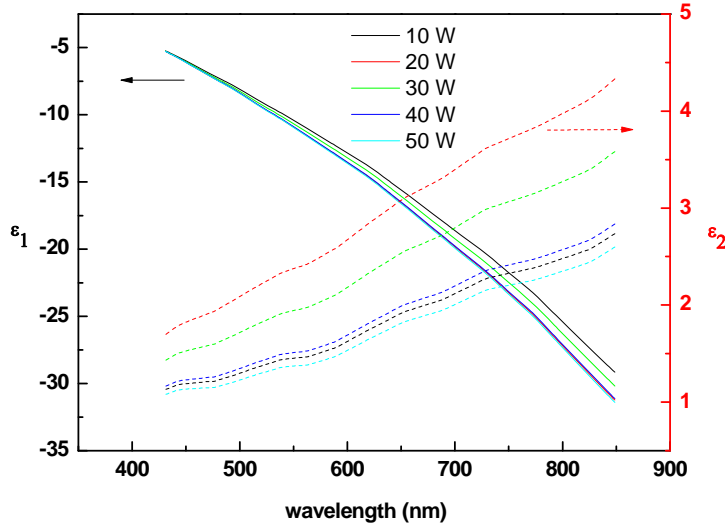

Fig.12. The dielectric constant of ε_1 (left) and ε_2 (right) of 50 nm-thick Ag thin film as a function of the forwarded dc power of 10, 20, 30, 40 and 50 W.

Our studies show that a dramatic improvement of surface roughness down to about 0.9 nm (rms) on the 50-nm-thick pure Ag film without a seed growth layer has been achieved. The ellipsometric results show that the variation of ε_1 and ε_2 of Ag films as function of the thickness from thin film to bulk. It is also shown that the real part of permittivity of ultra-thin Ag film became positive with the thickness reduced to 5 nm.

2.2.4 Dielectric films

The fabrication and characterization of dielectric films has been carried out recently. Heavy research on multilayer based hyperlens and other type of superlens will be started once the systematic results of the dielectric films are ready.

Conclusion

In conclusion, we have done simulations for metal/dielectric multilayer structures, their applications as hyperlens for sub-wavelength imaging with resolution beyond diffraction limit, optimized metal (silver) films and started fabrication and characterization of dielectric films with in-situ ellipsometry monitoring the thickness and optical constants. We numerically demonstrated that three dimensional imaging hyperlens with resolution of about 75 nm could be achieved. We also simulated multilayer structures for other superlens applications. In the experimental aspect, we have systematically investigated silver films fabricated at different preparation conditions and effects of thickness on their properties. High quality silver films with root-mean-square roughness of about 0.9 nm were achieved. We also found that the dielectric constant of the silver films are sensitive to the thickness and the real part of the constant become positive when the silver film is as thin as 5 nm, which is very important to the application of the silver films in nanophotonic devices including superlens for high resolution imaging. In addition, the fabrication and characterization for dielectric films has also carried out. Multilayer hyperlens and other type of superlens will be fabricated and characterized once the characterization of the dielectric film is completed.

Publication list

1. DongDong LI, D. H. ZHANG* and C.C. YAN, "Two-dimensional sub-wavelength imaging with a hemispherical hyperlens", The 5th International Conference on Nanophotonics (ICNP), 22-26, 2011 and to be published in Applied Optics.

2. Haijiao BIAN, Dao Hua ZHANG, Dongdong LI, Yueke WANG, Zhengji XU, "Surface Roughness and Optical Constants of dc Magnetron Sputtered Silver Films", ICMAT, Singapore, 26 June-1 July, 2011. To be published in Applied Physics A.